CONF-781055--5

A SUPERCONDUCTING DIPOLE MAGNET FOR THE UTSI MHD FACILITY

S-T. Wang, R. C. Niemann, L. R. Turner, L. Genens, W. Pelczarski,
J. Gonczy, J. Hoffman, Y-C. Huang, N. Modjeski, and E. Kraft

Prepared for

Applied Superconductivity Conference
Pittsburgh, PA
September 25-28, 1978

U of C-AUA-USDOE

ARGONNE NATIONAL LABORATORY, ARGONNE, ILLINOIS

Operated under Contract W-31-109-Eng-38 for the
U. S. DEPARTMENT OF ENERGY

DISCLAIMER

The facilities of Argonne National Laboratory are owned by the United States Government. Under the terms of a contract (W-31-109-Eng-38) between the U. S. Department of Energy, Argonne Universities Association and The University of Chicago, the University employs the staff and operates the Laboratory in accordance with policies and programs formulated, approved and reviewed by the Association.

MEMBERS OF ARGONNE UNIVERSITIES ASSOCIATION

The University of Arizona
Carnegie-Mellon University
Case Western Reserve University
The University of Chicago
University of Cincinnati
Illinois Institute of Technology
University of Illinois
Indiana University
Iowa State University
The University of Iowa
Kansas State University
The University of Kansas
Loyola University
Marquette University
Michigan State University
The University of Michigan
University of Minnesota
University of Missouri
Northwestern University
University of Notre Dame
The Ohio State University
Ohio University
The Pennsylvania State University
Purdue University
Saint Louis University
Southern Illinois University
The University of Texas at Austin
Washington University
Wayne State University
The University of Wisconsin

A SUPERCONDUCTING DIPOLE MAGNET FOR THE UTSI MHD FACILITY

S-T. Wang, R. C. Niemann, L. R. Turner, L. Genens, W. Pelczarski, J. Gonczy, J. Hoffman, Y.-C. Huang, N. Modjeski, and E. Kraft*

ABSTRACT

The Argonne National Laboratory is designing and will build a large superconducting dipole magnet system for use in the Coal Fired Flow MHD Research Facility at the University of Tennessee Space Institute (UTSI). Presented in detail are the conceptual design of the magnet geometry, conductor design, cryostability evaluation, magnetic pressure computation, structural design, cryostat design, and the cryogenics system design.

I. INTRODUCTION

The UTSI Superconducting Magnet System (UTSI SCMS) will consist of the superconducting magnet, magnet cryostat, a complete helium liquefier/refrigeration cryogenic facility, a magnet power supply, an integrated instrumentation and control system including a computer for magnet operation, data acquisition, system status and diagnosis, and magnet protection.

The UTSI SCMS will have an on-axis peak field of 6 T with an MHD channel warm aperture of 80 cm diameter at MHD channel inlet and of 100 cm diameter at the end of the effective field. The on-axis field profile is shown in Fig. 1. The effective field, defined as 4.8 T at inlet and 4.8 T at outlet, will have a field length of 3.0 m.

The UTSI SCMS will consist of fourteen layers of circular saddle coils. The layer thickness will be 3.8 cm and the winding build will be 0.53 m. Significant magnet system parameters are listed in Table I.

It is recognized that the UTSI SCMS must serve as a model with the design scalable to future large MHD magnets to be used in the Engineering Test Facility (ETF) and in the full-size base load systems. The successful experiences gained in designing and fabricating the U.S. SCMS[1] are carefully examined, utilized, and extended to improve the construction technique and to increase the reliability of the magnet performances.

TABLE I
Magnet System Parameters

On-Axis MHD Field	Inlet at 4.8 T, Peak at 6 T, Outlet at 4.8 T
Effective Magnetic Length	3.0 m
Ripple Along Field Tape	± 2.5% of On-Axis Field
Cross-Sectional Field Uniformity	± 5% of On-Axis Field
Coil Winding Bore (Smallest)	119 cm
Coil Bore Tube Thickness (Thickest)	∿ 6.3 cm
Winding Type	Circular Saddle with Intermediate Crossovers
Operational Current	4000 A
Peak Field	6.8 T
Winding Build	0.53 m
Layer Thickness	3.8 cm
No. of Layers	14
Ampere Turns	4000 x 3620
Total Conductor Length	39,000 m
Average Current Density	∿ 3300 A/cm^2 in Copper 2000 A/cm^2 in Winding
Cryostability	0.135 W/cm^2
Stored Energy	168 MJ
Inductance	21 H
Maximum Transverse Force	29,706 kg/cm
4.2 K Cold Mass Weight	124,078 kg
4.2 K Cold Mass Dimensions	∿ 3.1 m dia.x5.1 m long
Vacuum Vessel Dimensions	∿ 3.6 m dia.x6.4 m long
Total Magnet Weight	∿ 156,348 kg

Manuscript received September 28, 1978

*Work supported by the U. S. Department of Energy
Argonne National Laboratory, Argonne, IL USA

II. COIL CONFIGURATION AND LAYER STRUCTURE

The coil configuration and field profile are shown in Fig. 1. The magnet is of the circular saddle shape with fourteen layers. The cross section of the coils is chosen such that the ampere-turns are efficient while reducing the azimuthal force buildup on the inner layers.

A Micarta coil form similar to the one used for the U.S. SCMS coil fabrication is planned for the saddle coil. The coil form will be 3.1 cm thick and slotted to allow it to conform to the substrate circumference. The slots will be filled with glass beads and epoxy to sustain the curved shape.

The layer structure is shown in Fig. 2. Experience with the U.S. SCMS magnet fabrication has shown that saddle coils are best assembled by spiral banding. Therefore, each layer of coils will be assembled on the bore tube by spiral banding of 3.8 cm pitch length. The banding will cover 50% of the coil surface. The banding proposed will be 1.525 cm x 0.35 cm 7075-T6 aluminum alloy. Since the burst force shall be taken by ring girders instead of bore tube, the banding will be strong enough for coil assembly but too weak to transmit the burst force to the bore tube. The banding will be insulated with either Formvar coating or Mylar tape. The banding insulation will be reinforced further with 0.175 cm thick U-shaped pultruded fiberglass. For the coil end region, Micarta blankets 0.175 cm thick will replace the U-shaped pultruded fiberglass. The blanket will be slotted like the fingers of an outspread hand in order to provide free-flow liquid helium channels in the coil end region.

III. CONDUCTOR DESIGN AND TURN-TO-TURN INSULATION

An operating current of 4000 A is chosen to minimize both the winding cost and the induced voltage in the winding should the magnet become normal and also to keep the heat leak requirements comparable with cryostat heat leak.

As shown in Fig. 3, the selected conductor will be 3.10 cm high with conductor thickness varying according to field grades. The turn-to-turn insulation will be pultruded fiberglass with keystoned cross section as shown in Fig. 3. The keystoned feature eliminates the tedious labor of inserting correction wedges during the coil winding and assures better saddle coil quality than the U.S. SCMS.

A peak field of 6.8 T occurs on the innermost layer of the magnet, on the saddle of subcoil 1A (see Fig. 2) which is near the high field cross section.

The conductor will be graded into three grades. The high field grade with a short sample of 4500 A at 7.5 T will cover conductor with 6.8 T peak field. The medium field grade, with a short sample of 4500 A at 6.5 T, will cover 6.0 T peak field and the low field grade, 4500 A at 4.5 T, will cover 4.0 T peak field. The current density in the conductor, at 4000 A, is 3140 A/cm^2, 3310 A/cm^2, and 3450 A/cm^2 for high field grade, medium field grade, and low field grade, respectively. The overall current density in the coils is assumed to be 2000 A/cm^2 in the field computation.

IV. CRYOSTABILITY EVALUATIONS

The design of conductor, turn-to-turn insulation, and layer structure allows a 50% edge cooling and more than 50% internal face cooling. The conductor is cryostable with a required steady state heat transfer of 0.14 W/cm^2. This low heat flux assures the unconditional stability for the UTSI SCMS superconductor.

The cryostability of the conductor is enhanced by the cooling channels. Recovery current for two conductors was studied. With the same amount of superconductor and otherwise the same except for the height of 2.54 cm and 3.10 cm, the computation ignores turn-to-turn heat transfer, which should make the recovery current even higher.

Further calculations show that the 3.10 cm high conductor is absolutely cryostable with a recovery current of 4080 A; that is, with such a current, the conductor will recover from a perturbing heat flux of any given magnitude and any extent in space and time. This absolute stability assumes an adequate replenishment of liquid helium coolant; recent experiments at Argonne[2] suggest that adequate replenishment does in fact occur. Under various conditions, the recovery currents for both the absolute stability and conditional stability are computed as shown in Fig. 4.

V. MAGNETIC FORCES AND MAGNETIC PRESSURES

The conductor in the high field cross section A-A in Fig. 2 exerts a force of 30,000 kg/cm outward on the girders; a force of 26,385 kg/cm pushes the two halves of the magnet together. The radial magnetic pressure per 5° azimuthal increment totaled over 14 coils and the accumulated azimuthal pressure for each layer, calculated in the high field cross-section is shown in Figs. 5a and 5b, respectively.

A decentering force of 0.2 x 10^6 kg resulting from the asymmetric field distribution, is supported by the high field end flange and the step in the cold bore tube.

VI. MECHANICAL DESIGN

A series of outer ring girders form the containment structure for the lateral burst force. Each ring girder, as shown in Fig. 6, is made up of four circular segments, each subtending a 45° angle. These segments are connected to each other by pins utilizing an offset finger arrangement to interlace with adjacent segments and provide sufficient shear area of the pins.

The predominant stress in the ring girder sections is a bending stress. The bending of the ring girder causes its diameter parallel to the field direction to shorten. However, force transmission to the bore tube due to this shortening is avoided by providing a predetermined gap between part of the inner surface of the ring girder and the outer surface of the filler layer.

Over the effective field region, each of the eleven ring girders is made up of two stainless steel segments adjacent to the coil and two aluminum segments opposite to the coil. The cross section of the stainless steel segment is an I-beam, while that of the aluminum is a solid rectangle. The maximum stress in the peak field region is 2.4 x 10^6 N/m^2 (49 kpsi) in the stainless steel and 1.7 x 10^6 N/m^2 (35 kpsi) in the aluminum.

The bore tube, as shown in Fig. 6, will either be completely forged 316 L stainless steel or the forged 316 L stainless steel in the tube section and the end flange cast of 316 L from ACI Gr. CF3MA. The end flange is an annular plate reinforced with radial ribs and supported at the inner boundary by the bore tube. The bending moments transferred by the end flanges to the bore tube are supported by providing ribs on the bore tube section outside to the flange.

VII. CRYOSTAT, COLD MASS SUPPORT, COOLDOWN, CRYOGENICS

The cryostat will be designed with a liquid nitrogen shield and multilayer superinsulation. The heat leaks of the helium vessel will be 13.4 W. The 124 metric tons of cold mass is supported at each end by four epoxy fiberglass tension supports. The conceptual cryostat configuration is shown in Fig. 7, and the cryostat design criteria are listed in Table II.

The cold mass support system will employ low heat leak fiberglass composite tension member-type support. The support members will be heat intercepted at an intermediate point by thermal connection to the thermal radiation shield. The support system will be configured with four support hangers affixed to each end of the extended cold bore tube. The connection to the cold bore tube will be by means of an extension of the cold bore tube. This eliminates the welding of support lugs during assembly and additional loading of the end flanges.

In order to avoid the development of potentially high thermal stresses due to differential contraction, during cooldown and warmup, between the high mass cold bore tube and coil assembly and the relatively low mass helium vessel shell, the rigid end flange of the helium vessel will be terminated at the outer boundary of the coil assembly and a thin shell will then connect the outer shell of the helium vessel. The thin shell will act as a membrane and will flex to compensate for possible differential contraction. In addition, the thin shell will have formed into it during manufacture an annular corrugation for enhanced axial flexure.

A refrigerator/liquefier will be employed to cool down the magnet cold mass from 300 K to approximately 15 K, to initially fill the helium vessel by direct transfer to the helium vessel and to provide liquid for the steady state operation of the magnet system. The refrigeration capacity will be as required by the magnet cooldown period. The liquefication capacity will be 50 L/hr; i.e., approximately three times the estimated total LHe^4 average use rate. Multiple compressors will be employed to provide for maintenance and operating downtime periods.

The liquid for the steady state operation of the magnet system will be stored in and transferred from a single intermediate LHe^4 dewar. The dewar will be equipped to receive liquid from the refrigerator/liquefier and external supply dewars. The capacity will be 7500 L; i.e., approximately 1.6 times the magnet cryostat LHe^4 inventory.

Cold bore tube and coil assembly will be cooled by supplying gas to four axial distribution manifolds located on the surface of the bore tube. The cooling will then be by outward gas conduction through the helium channels in the conductor. The ring girders will be cooled through tubes imbedded in or otherwise in good thermal contact with the girders. Manifolding will permit the cooling helium gas to be divided among the coil region and the girders as required.

VIII. POWER SUPPLY INSTRUMENTATION AND CONTROL

The magnet power supply will have an output characteristic of 20 V-4000 A. A 0.05 Ω dump resistor submerged in a water tank will be used to safely discharge the 168 MJ magnet energy in the event of emergency. Therefore, the fast-time constant for charge will be about 70 min and the fast-time constant for discharge will be 7 min. The maximum discharge terminal voltage will be 100 V with respect to the grounding center tap of the energy dump resistor.

The system will incorporate an integrated control system. The control system will provide functions for

both normal operation and the various fault conditions. A computer will be employed to permit programming of cooldown, magnet energization, etc. A data logging feature will be included along with facilities for data storage, transmission, and printout.

Parameters to be maintained include the following: Voltages within the magnet, current, accelerations, temperatures, gas flow rates, cryogenic system operating points, liquid levels, and structural loading.

TABLE II
UTSI SCMS Cryostat Parameters

I.	He^4 Vessel	
	A. Design Pressures	2.45×10^5 N/m^2 (50 psi) internal, 1.03×10^5 N/m^2 (15 psi) external and 2.07×10^5 N/m^2 (30 psi) at device relief
	B. Weight	Total 124,078 kg
	1. Conductor	40,905 kg
	2. Bore tube and end flanges	11,817 kg
	3. Ring girders	50,000 kg
	4. Helium vessel outer shell	7,090 kg
	5. Coil form, coil end filler and blankets	7,135 kg
	6. Banding	1,363 kg
	7. Insulator	1,227 kg
	C. Heat Loads	13.4 W or 19 L/h
	D. Liquid Helium Inventory	4710 L
II.	Thermal Radiation Shield	
	A. Type	Conduction cooled with load into LN_2 reservoir multilayer insulation on both sides
	B. Weight	2000 kg
	C. Heat Loads	135 W or 3.2 L/hr
	D. Material	304 SST and copper
III.	Vacuum Vessel and Support	
	A. Design Pressures	1.38×10^5 N/m^2 (20 psi) internal, 1.03×10^5 N/m^2 (15 psi) external and 1.38×10^5 N/m^2 (20 psi) internal pressure emergency vent
	B. Weight	30,270 kg
	C. Material	304 SST
IV.	Dynamic Loading	
	A. Operating	
	1. 3 g vertically down	
	2. 1 g vertically up	
	3. ±1 g lateral	
	4. ±1 g axial	
	B. Shipping	
	1. ±1 g vertical	
	2. ±1 g lateral	
	3. ±1 g axial	

REFERENCES

1. S-T. Wang, R. C. Niemann, R. L. Kustom, P. Smelser, W. J. Pelczarski, L. R. Turner, E. W. Johnson, E. F. Kraft, S. H. Kim, J. D. Gonczy, H. F. Ludwig, K. F. Mataya, W. E. LaFave, F. J. Lawrentz, and F. P. Catania, "Fabrication Experiences and Operating Characteristics of the U.S. SCMS Superconducting Dipole Magnet for MHD Research," Advances in Cryogenic Engineering Conference, Vol. 23, pp. 17-27 (1978).

2. J. Harrang, S-T. Wang, Y-C. Huang, L. R. Turner, and J. W. Dawson, "Stability Simulation of Cryostable Superconductors Under Transient Mechanical Perturbations," (to be submitted to this Conference).

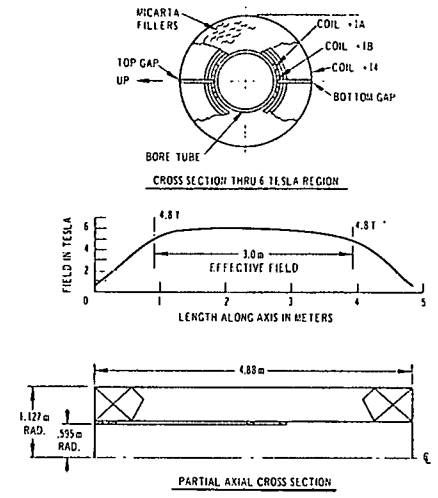

Fig. 1. Coil configuration and axial field profiles.

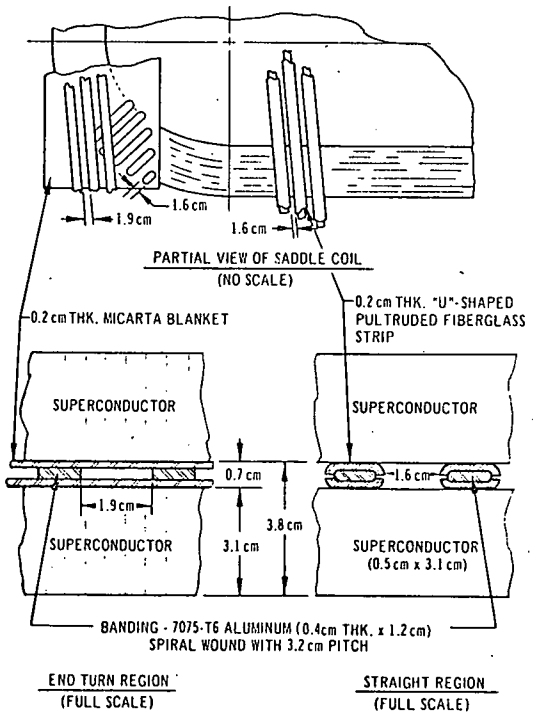

Fig. 2. Layer structure.

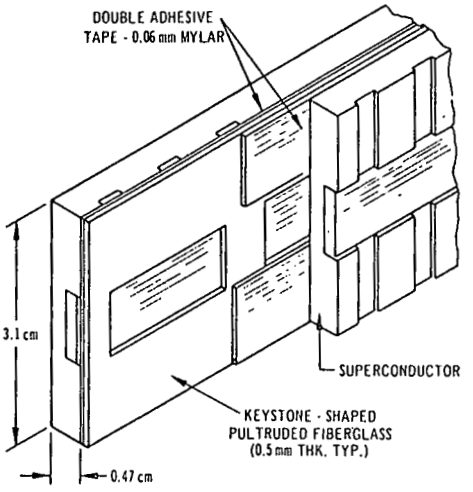

Fig. 3. Conductor and overall turn-to-turn insulation.

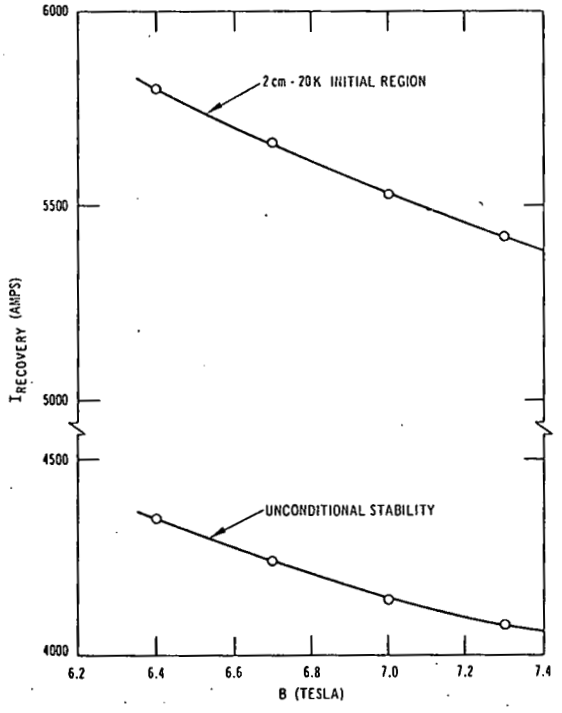

Fig. 4. Conditional recovery current and absolute recovery current.

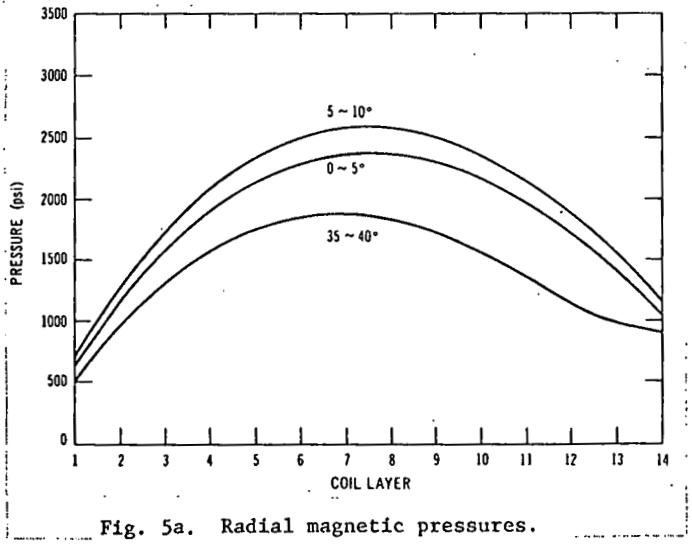

Fig. 5a. Radial magnetic pressures.

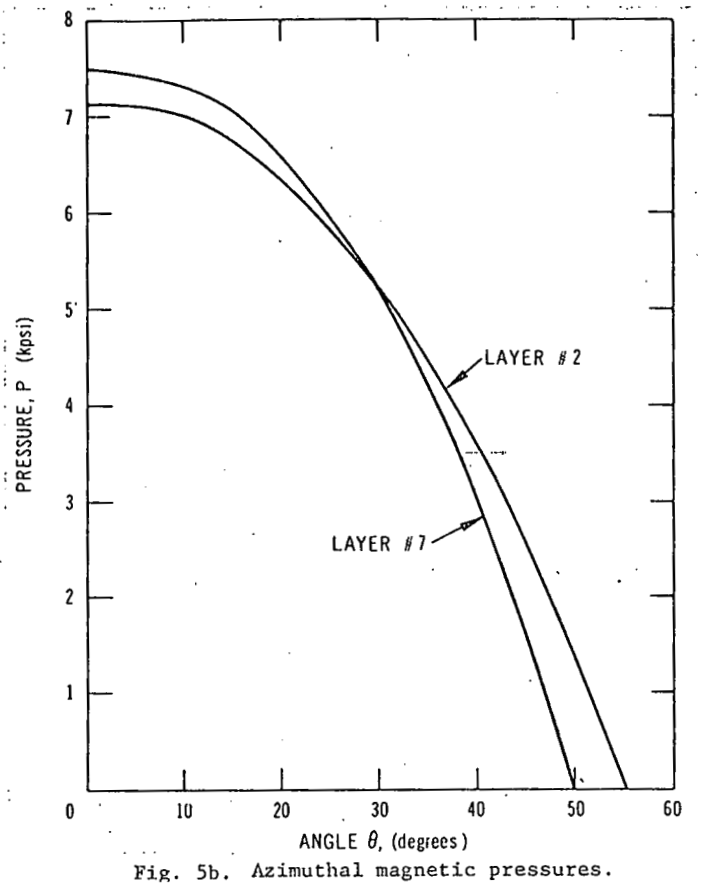

Fig. 5b. Azimuthal magnetic pressures.

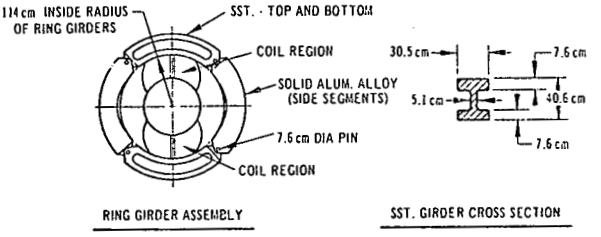

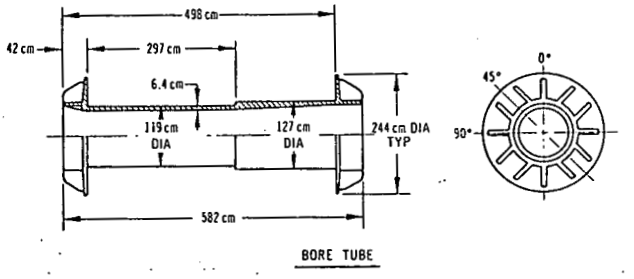

Fig. 6. Ring Girders and Bore Tube.

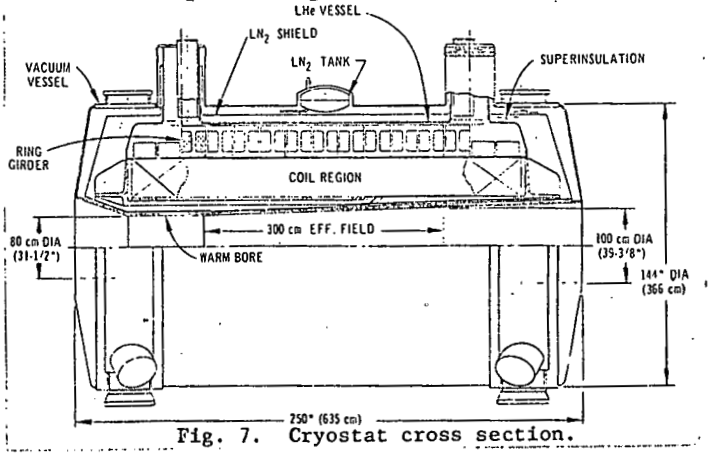

Fig. 7. Cryostat cross section.